

# DISK WINDS AND THE ACCRETION–OUTFLOW CONNECTION

ARIEH KÖNIGL

*Department of Astronomy & Astrophysics, University of Chicago  
Chicago, IL 60637, USA*

and

RALPH E. PUDRITZ

*Department of Physics and Astronomy, McMaster University  
Hamilton, Ontario L8S 4M1, Canada*

We review recent observational and theoretical results on the relationship between circumstellar accretion disks and jets in young stellar objects. We then present a theoretical framework that interprets jets as accretion-powered, centrifugally driven winds from magnetized accretion disks. Recent progress in the numerical simulation of such outflows is described. We also discuss the structure of the underlying magnetized protostellar disks, emphasizing the role that large-scale, open magnetic fields can play in angular momentum transport.

## I. INTRODUCTION

Two of the most remarkable aspects of star formation are the presence of disks and of energetic outflows already during the earliest phases of protostellar evolution. There is now strong evidence for an apparent correlation between the presence of outflows and of actively accreting disks, which suggests that there is a physical link between them. The prevalent interpretation is that the outflows are powered by accretion and that magnetic stresses mediate the inflow and outflow processes and eject some of the inflowing matter from the disk surfaces. If disks are threaded by open magnetic field lines then the outflows can take the form of centrifugally driven winds. Such highly collimated winds carry angular momentum and may, in principle, play an important role in the angular momentum budget of disks and their central protostars.

This review concentrates on the developments in the study of outflows and their relationship to circumstellar disks that have occurred since the publication of *Protostars and Planets III*. The reader may consult Königl and Ruden in that volume and Pudritz et al. (1991)

for reviews of earlier work. In Sec. II we summarize the observational findings on outflows, disks, and magnetic fields, and their implications. Sec. III deals with the general theory of magnetized outflows and Sec. IV describes numerical simulations of disk-driven MHD winds. In Sec. V we consider the theory of magnetized protostellar disks. Our conclusions are presented in Sec. VI.

## II. OBSERVATIONAL BACKGROUND

### A. Bipolar Outflows and Jets

Bipolar molecular outflows and narrow atomic jets are ubiquitous phenomena in protostars. There are now more than 200 bipolar CO sources known (see chapter by Richer et al.): they typically appear as comparatively low-velocity ( $\lesssim 25 \text{ km s}^{-1}$ ) and moderately collimated (length-to-width ratios  $\sim 3 - 10$ ) lobes, although several highly collimated CO outflows that exhibit high velocities ( $> 40 \text{ km s}^{-1}$ ) near the flow axis have now been detected. The mass outflow rate exhibits a continuous increase with the bolometric luminosity of the driving source for  $L_{\text{bol}}$  in the range  $\sim 1 - 10^6 L_{\odot}$ . Molecular outflows are present through much of the embedded phase of protostars and, in fact, appear to be most powerful and best collimated during the earliest (Class 0) protostellar evolutionary phase (Bontemps et al. 1996).

The bipolar lobes are generally understood to represent ambient molecular material that has been swept up by the much faster, highly supersonic jets that emanate from the central star/disk system (see chapters by Eislöffel et al. and by Hartigan et al.). Jets associated with low-luminosity ( $L_{\text{bol}} < 10^3 L_{\odot}$ ) young stellar objects (YSOs) have velocities in the range  $\sim 150 - 400 \text{ km s}^{-1}$ , large ( $> 20$ ) Mach numbers, and can have opening angles as small as  $\sim 3 - 5^{\circ}$  on scales of  $10^3 - 10^4 \text{ AU}$ . The inferred mass outflow rates are  $\sim 10^{-10} - 10^{-8} M_{\odot} \text{ yr}^{-1}$ . A significant number of outflows has also been detected by optical observations of intermediate-mass ( $2 \lesssim M_{*}/M_{\odot} \lesssim 10$ ) Herbig Ae/Be stars and other high-luminosity sources (Mundt and Ray 1994; Corcoran and Ray 1997). The jet speeds and mass outflow rates in these YSOs are, respectively, a factor  $\sim 2 - 3$  and  $\sim 10 - 100$  higher than in low- $L_{\text{bol}}$  objects. The total momentum delivered by the jets, taking into account both the density corrections implied by their partial ionization state and the long lifetimes indicated by the detection of pc-scale outflows, appears to be consistent with that measured in the associated CO outflows (e.g., Hartigan et al. 1994; Eislöffel and Mundt 1997). A critical review of the physical mechanisms of coupling the jets and the surrounding gas is given in Cabrit et al. (1997).

The momentum discharge deduced from the bipolar-outflow observations is typically a factor  $\sim 10^2$  higher than the radiation-pressure thrust  $L_{\text{bol}}/c$  produced by the central source (e.g., Lada 1985), which

rules out radiative acceleration of the jets. Since the bolometric luminosity of protostars is by and large due to accretion, and since the ratio of jet kinetic luminosity to thrust is of order the outflow speed ( $\sim 10^{-3} c$ ), it follows that the jet kinetic luminosity is on average a fraction  $\sim 0.1$  of the rate at which gravitational energy is liberated by accretion. This high ejection efficiency is most naturally understood if the jets are driven magnetically.

Magnetic fields have also been implicated in jet collimation. A particularly instructive case is provided by *HST* observations of the prototypical disk/jet system HH 30 (Burrows et al. 1996). The jet in this source can be traced to within  $\lesssim 30$  AU from the star and appears as a cone with an opening angle of  $3^\circ$  between 70 and 700 AU. The narrowness of the jet indicates some form of intrinsic collimation since external density gradients would not act effectively on these small scales. Magnetic collimation is a likely candidate, made even more plausible by the fact that the jet appears to recollimate: its apparent opening angle decreases to  $1.9^\circ$  between 350 and  $10^4$  AU. Similar indications of recollimation have also been found in other jets. Given that any inertial confinement would be expected to diminish with distance from the source, this points to the likely role of intrinsic magnetic collimation.

## B. Connection with Accretion Disks

The evidence for disks around YSOs and for their link to outflows has been strengthened by a variety of recent observations. These include systematic studies of the frequency of disks by means of infrared and millimeter surveys and further interferometric mappings (now comprising also the submillimeter range) that have resolved the structure and velocity field of disks down to scales of a few tens of AU (see chapter by Wilner and Lay). High-resolution images of disks in several jet sources have also been obtained in the near-infrared using adaptive optics and in the optical using the *HST* (see chapter by McCaughrean et al.).

Stellar jets are believed to be powered by the gravitational energy liberated in the accretion process and to be fed by disk material. This picture is supported by the strong apparent correlation that is found (e.g., Cabrit et al. 1990; Cabrit and André 1991; Hartigan et al. 1995) between the presence of outflow signatures (such as P Cyg line profiles, forbidden line emission, thermal radio radiation, or well-developed molecular lobes) and accretion diagnostics (such as ultraviolet, infrared, and millimeter-wavelength emission excesses, or inverse P Cyg line profiles). Further support is provided by the apparent decline in outflow activity with stellar age, which follows the similar trend exhibited by the disk frequency (see chapters by André et al. and by Mundy et al.) and mass accretion rate (see chapter by Calvet et al.). While virtually every Class 0 source has an associated outflow, a survey of

optical and molecular outflows in the Taurus-Auriga cloud (Gomez et al. 1997) found an incidence rate of  $\gtrsim 60\%$  among Class I objects but only  $\sim 10\%$  among Class II ones (and none in Class III objects). The inference that jets are powered by accretion and originate in accretion disks is strengthened by the evidence for disks in the youngest YSOs in which outflows are detected. For example, sub-mm interferometric observations of VLA 1623, one of the youngest known Class 0 sources, imply the presence of a circumstellar disk of radius  $< 175$  AU and mass  $\geq .03 M_{\odot}$  (Pudritz et al. 1996).

Corcoran and Ray (1998) demonstrated that the correlation between [OI] $\lambda 6300$  line luminosity (an outflow signature) and excess infrared luminosity (an accretion diagnostic) originally found in Class II sources extends smoothly to YSOs with masses of up to  $\sim 10 M_{\odot}$  and spans 5 orders of magnitude in luminosity. It is noteworthy that correlations of the type  $\dot{M} \propto L_{\text{bol}}^{0.6}$  that apply to both low-luminosity and high-luminosity YSOs have been established in several independent studies for the mass *accretion* rate (from IR continuum measurements; Hillenbrand et al. 1992 – see, however, Hartmann et al. 1993, Bell 1994, Miroshnichenko et al. 1997, and Pezzuto et al. 1997 for alternative interpretations of the infrared emission in Herbig Ae/Be stars), the *ionized* mass *outflow* rate in the jets (from radio continuum observations; Skinner et al. 1993), and the bipolar *molecular outflow* rate (from CO line measurements; Levreault 1988). Taken together, these relationships suggest that a strong link between accretion and outflow exists also in high-mass YSOs and that the underlying physical mechanism is basically the same as in low-mass objects (see Königl 1999).

Strong evidence for a disk origin of jets is available for the energetic outflows associated with FU Orionis outbursts (see chapters by Bell et al. and by Calvet et al.). The outbursts have been inferred to arise in young YSOs that are still rapidly accreting, although it is possible that they last into the Class II phase. The duration of a typical outburst is  $\sim 10^2$  yr, and during that time the mass accretion rate (as inferred from the bolometric luminosity) is  $\sim 10^{-4} M_{\odot} \text{ yr}^{-1}$ , with the deduced mass outflow rate  $\dot{M}_{\text{wind}}$  (at least in the most powerful sources like FU Ori and Z CMa) being a tenth as large. The ratio  $\dot{M}_{\text{wind}}/\dot{M}_{\text{acc}} \approx 0.1$  is similar to that inferred in Class II YSOs and again points to a rather efficient outflow mechanism. Detailed spectral modeling demonstrates that virtually all the emission during an outburst is produced in a rotating disk. Furthermore, the correlation found in the prototype FU Ori between the strength and the velocity shift of various photospheric absorption lines can be naturally interpreted in terms of a wind accelerating from the disk surface (Calvet et al. 1993; Hartmann and Calvet 1995). Because of the comparatively low temperatures ( $\sim 6000$  K) in the wind acceleration zone, thermal-pressure and radiative driving are unimportant (the latter due to the lack of a high-temperature source):

magnetic driving is thus strongly indicated. The recurrence time of outbursts has been estimated to lie in the range  $\sim 10^3 - 10^4$  yr, and if these outbursts are associated with the large-scale bow shocks detected in pc-scale jets (e.g., Reipurth 1991), then a value near the lower end of the range is implied. In that case most of the stellar mass would be accumulated through this process, and, correspondingly, most of the mass and momentum ejected over the lifetime of the YSO would originate in a disk-driven outflow during the outburst phases (Hartmann 1997).

### C. Magnetic Fields in Outflow Sources

The commonly accepted scenario for the origin of low-mass protostars is that they are produced from the collapse of the inner regions of molecular clouds that are supported by large-scale magnetic fields (and likely also hydromagnetic waves). In this picture, a gravitationally unstable inner core forms as a result of mass redistribution by ambipolar diffusion and subsequently collapses dynamically (see review by McKee et al. 1993). The mass accretion rates predicted by this picture are consistent with the inferred evolution of young YSOs (e.g., Ciolek and Königl 1998). Basic support for this scenario is provided by far-infrared (e.g., Hildebrand et al. 1995) and sub-mm (e.g., Greaves et al. 1994, 1995; Schleuning 1998; Greaves and Holland 1998) polarization measurements, that reveal an ordered, hourglass-shaped field morphology on sub-pc scales consistent with the field lines being pulled in at the equatorial plane of the contracting core. Moreover, H I and OH Zeeman measurements (e.g., Crutcher et al. 1993, 1994, 1996) are consistent with the magnetic field having the strength to support the bulk of the cloud against gravitational collapse.

There now exist measurements of magnetic fields in the flows themselves at large distances from the origin (see chapter by Eisloffel et al.). In particular, the strong circular polarization detected in T Tau S in two oppositely directed nonthermal emission knots separated by 20 AU indicates a field strength of at least several gauss (Ray et al. 1997). This high value can be attributed to a magnetic field that is advected from the origin by the associated stellar outflow and that dominates the internal energy of the jet. This observation thus provides direct evidence for the essentially hydromagnetic character of jets.

## III. MHD WINDS FROM ACCRETION DISKS

### A. Basic MHD Wind Theory

The theory of centrifugally driven winds was first formulated in the context of rotating, magnetized stars (Schatzmann 1962; Weber and Davis 1967; Mestel 1968). Using 1-D, axisymmetric models, it was shown that such stars could lose angular momentum by driving winds

of this type. This idea was applied to magnetized accretion disks in the seminal paper of Blandford and Payne (1982, BP). Every annulus of a Keplerian disk may be regarded as rotating close to its “breakup” speed, so disks are ideal drivers of outflow when sufficiently well magnetized. The removal of disk angular momentum allows matter to move inward and produces an accretion flow. In a steady state, field lines must also slip radially out of the accreting gas and maintain their fixed position in space: this necessitates diffusive processes. As we discuss in Sec. V.B, strong field diffusivity is a natural attribute of the partially ionized regions of protostellar disks, and it could counter both the advection of the field lines by the radial inflow and their winding-up by the differential rotation in the disk.

Consider, for the moment, the simplest possible description of a magnetized, rotating gas threaded by a large-scale, open field (characterized by an even symmetry about the midplane  $z = 0$ ). The equations of stationary, axisymmetric, ideal MHD are the conservation of mass (continuity equation); the equation of motion with conducting gas of density  $\rho$  subject to forces associated with the pressure  $P$ , the gravitational field (from the central object whose gravitational potential is  $\phi$ ), and the magnetic field  $\mathbf{B}$ ; the induction equation for the evolution of the magnetic field in the moving fluid; and the solenoidal condition on  $\mathbf{B}$ :

$$\nabla \cdot (\rho \mathbf{V}) = 0, \quad (1)$$

$$\rho \mathbf{V} \cdot \nabla \mathbf{V} = -\nabla p - \rho \nabla \phi + \frac{1}{4\pi} (\nabla \times \mathbf{B}) \times \mathbf{B}, \quad (2)$$

$$\nabla \times (\mathbf{V} \times \mathbf{B}) = 0, \quad (3)$$

$$\nabla \cdot \mathbf{B} = 0. \quad (4)$$

Consider the **angular momentum equation** for axisymmetric flows. This is described by the  $\phi$  component of equation (2). Ignoring stresses that would arise due to turbulence, and noting that neither the pressure nor the gravitational term contributes, one finds that

$$\rho \mathbf{V}_p \cdot \nabla (r V_\phi) = \frac{\mathbf{B}_p}{4\pi} \cdot \nabla (r B_\phi), \quad (5)$$

where we have broken the magnetic and velocity fields into poloidal and toroidal components:  $\mathbf{B} = \mathbf{B}_p + B_\phi \hat{\mathbf{e}}_\phi$  and  $\mathbf{V} = \mathbf{V}_p + V_\phi \hat{\mathbf{e}}_\phi$ .

Important links between the velocity field and the magnetic field are contained in the induction equation (3), whose solution is

$$\mathbf{V} \times \mathbf{B} = \nabla \psi, \quad (6)$$

where  $\psi$  is some scalar potential. This shows that the electric field due to the bulk motion of conducting gas in the magnetic field is derivable from an electrostatic potential. This has two important ramifications. The first is that, because of axisymmetry, the toroidal component of this equation must vanish ( $\partial\psi/\partial\phi = 0$ ). This forces the poloidal velocity vector to be parallel to the poloidal component of the magnetic field,  $\mathbf{V}_p \parallel \mathbf{B}_p$ . This, in turn, implies that there is a function  $k$ , the mass load of the wind, such that

$$\rho \mathbf{V}_p = k \mathbf{B}_p . \quad (7)$$

Substitution of this result into the continuity equation (1), and then use of the solenoidal condition (eq. [4]) reveals that  $k$  is a constant along a surface of constant magnetic flux, i.e., that it is conserved along field lines. This function can be more revealingly cast by noting that the wind mass loss rate passing through an annular section of the flow of area  $dA$  through the flow is  $d\dot{M}_w = \rho V_p dA$ , while the amount of poloidal magnetic flux through this same annulus is  $d\Phi = B_p dA$ . Thus, the mass load per unit time and per unit magnetic flux, which is preserved along each streamline emanating from the rotor (a disk in this case), is

$$k = \frac{\rho V_p}{B_p} = \frac{d\dot{M}_w}{d\Phi} . \quad (8)$$

The mass load is determined by the physics of the underlying rotor, which is its source.

A second major consequence of the induction equation follows from the poloidal part of equation (6). Taking the dot product of it with  $\mathbf{B}_p$  and using equation (7), one easily proves that  $\psi$  is also a constant along a magnetic flux surface and that it must take the form  $\psi = \Omega - (k B_\phi / \rho r)$ . In order to evaluate  $\psi$ , note that  $B_\phi = 0$  at the disk midplane by the assumed even symmetry. Thus  $\psi$  equals  $\Omega_0$ , the angular velocity of the disk at the midplane. One thus has a relation between the toroidal field in a rotating flow and the rotation of that flow,

$$B_\phi = \frac{\rho r}{k} (\Omega - \Omega_0) . \quad (9)$$

Let us now examine the angular momentum equation. Returning to the full equation (5) and applying equation (7) and the constancy of  $k$  along a field line, one obtains

$$\mathbf{B}_p \cdot \nabla (r V_\phi - \frac{r B_\phi}{4\pi k}) = 0 . \quad (10)$$

Hence the angular momentum per unit mass,

$$l = r V_\phi - \frac{r B_\phi}{4\pi k} , \quad (11)$$

is constant along a streamline. This shows that the specific angular momentum of a magnetized flow is carried by both the rotating gas (first term) and the twisted field (second term). The value of  $l$  may be found by eliminating the toroidal field between equations (9) and (11) and solving for the rotation speed of the flow,

$$rV_\phi = \frac{lm^2 - r^2\Omega_o^2}{m^2 - 1}, \quad (12)$$

where the Alfvén Mach number  $m$  of the flow is defined as  $m^2 = V_p^2/V_A^2$ , with  $V_A = B_p/(4\pi\rho)^{1/2}$  being the Alfvén speed of the flow. The Alfvén surface is the locus of the points  $r = r_A$  on the outflow field lines where  $m = 1$ . The flow along any field line essentially corotates with the rotor until this point is reached. From the regularity condition at the Alfvén critical point (where the denominator of eq. [12] vanishes) one infers that the conserved specific angular momentum satisfies

$$l = \Omega_0 r_A^2. \quad (13)$$

If we imagine following a field line from its footpoint at a radius  $r_0$ , the Alfvén radius is at a distance  $r_A(r_0)$  from the rotation axis and constitutes the lever arm for the back torque that this flow exerts on the disk. The other critical points of the outflow are where the outflow speed  $V_p$  equals the speed of the slow and fast magnetosonic modes in the flow (at the so-called SM and FM surfaces).

Finally, a generalized version of Bernoulli's equation may be derived by taking the dot product of the equation of motion with  $\mathbf{B}_p$ . One then finds that the specific energy

$$E = \frac{1}{2}(V_p^2 + \Omega^2 r^2) + \phi + h + \Omega_0(\Omega_0 r_A^2 - \Omega r^2), \quad (14)$$

where  $h$  is the enthalpy per unit mass, is also a field-line constant.

The terminal speed  $V_p = V_\infty$  corresponds to the region where the gravitational potential and the rotational energy of the flow are negligible. Since for cold flows the specific enthalpy may be ignored, one infers from equation (14)

$$V_\infty \simeq 2^{1/2}\Omega_0 r_A, \quad (15)$$

a result first obtained by Michel (1969) for 1-D flows. The important point regarding outflow speeds from disks is that  $V_\infty/\Omega_0 r_0 \approx 2^{1/2}r_A/r_0$ : the asymptotic speed is larger than the rotor speed by a factor that is approximately the ratio of the lever arm to the footpoint radius.



## B. Connection with Underlying Accretion Disk

We now apply the angular momentum conservation relation (5) to calculate the torque exerted on a thin accretion disk by the external magnetic field. The vertical flow speed in the disk is negligible, so only the radial inflow speed  $V_r$  and the rotation speed  $V_\phi$  (Keplerian for thin disks) contribute. On the right-hand side, both the radial and vertical magnetic contributions come into play, so

$$\frac{\rho V_r}{r_0} \frac{\partial(r_0 V_\phi)}{\partial r_0} = \frac{B_r}{4\pi r_0} \frac{\partial(r_0 B_\phi)}{\partial r_0} + \frac{B_z}{4\pi} \frac{\partial B_\phi}{\partial z}. \quad (16)$$

One sees that specific angular momentum is removed from the inward accretion flow by the action of two types of magnetic torque. The first term on the r.h.s. represents radial angular momentum associated with the radial shear of the toroidal field, while the second term is vertical transport due to the vertical shear of the toroidal field. In a thin disk, and for typical field inclinations, the second term will dominate. Note that the first term vanishes at the disk midplane because  $B_r = 0$  there. Now, following standard thin-disk theory, vertical integration of the resulting equation gives a relation between the disk accretion rate,  $\dot{M}_{\text{acc}} = -2\pi\Sigma V_r r_0$ , and the magnetic torques acting on its surfaces (subscript s),

$$\dot{M}_{\text{acc}} \frac{d(r_0 V_\phi)}{dr_0} = -r_0^2 B_{\phi,s} B_z, \quad (17)$$

Angular momentum is thus extracted out of disks threaded by open magnetic fields. The angular momentum can be carried away either by toroidal Alfvén waves or, when the magnetic field lines are inclined by more than  $30^\circ$  from the vertical, by a centrifugally driven wind. By rewriting equation (11) as  $rB_\phi = 4\pi k(rV_\phi - l)$  and using the derived relations for  $k$  and  $l$ , the disk angular momentum equation can be cast into its most fundamental form,

$$\dot{M}_{\text{acc}} \frac{d(\Omega_0 r_0^2)}{dr_0} = \frac{d\dot{M}_{\text{wind}}}{dr_0} \Omega_0 r_A^2 (1 - (r_0/r_A)^2). \quad (18)$$

This equation shows that there is a crucial link between the mass outflow in the wind and the mass accretion rate through the disk:

$$\dot{M}_{\text{acc}} \simeq (r_A/r_0)^2 \dot{M}_{\text{wind}}. \quad (19)$$

One has arrived at the profoundly useful expression of the idea that, if viscous torques in the disk are relatively unimportant, the rate at which the disk loses angular momentum ( $\dot{j}_d = \dot{M}_{\text{acc}} \Omega_0 r_0^2$ ) is exactly the rate at which it is carried away by the wind ( $\dot{j}_w = \dot{M}_{\text{wind}} \Omega_0 r_A^2$ ).

The value of the ratio  $r_A/r_0$  is  $\sim 3$  for typical parameters, so one finds  $\dot{M}_{\text{wind}}/\dot{M}_{\text{acc}} \simeq 0.1$ , which is in excellent agreement with the

observations (Sec. II). The explanation of this relationship is thus intimately linked to the disk’s angular momentum loss to the wind.

### C. Flow Initiation and Collimation

Stellar winds usually require hot coronae to get started, while winds from disks, which effectively rotate near “breakup,” do not. In the case of a thin disk even a cool atmosphere will suffice as long as the field lines emerging from the disk make an angle  $\leq 60^\circ$  to the surface. This follows from Bernoulli’s equation by comparing the variations in the effective gravitational potential and the kinetic energy of a particle that moves along a field line near the disk surface (BP; Königl and Ruden 1993; Spruit 1996; but see Ogilvie and Livio 1998).

The collimation of an outflow, as it accelerates away from the disk, arises to a large extent from the hoop stress of the toroidal field component. From equation (9) one sees that at the Alfvén surface  $|B_\phi| \simeq B_p$  and that in the far field (assuming that the flow opens up to radii  $r \gg r_A$ )  $B_\phi/B_p \simeq r/r_A$ . Thus, the inertia of the gas, forced to corotate with the outflow out to  $r_A$ , causes the jet to eventually self-collimate through the  $\mathbf{j}_z \times \mathbf{B}_\phi$  force, which is known as the z-pinch in the plasma physics literature.

The detailed radial structure of the outflow is deduced by balancing all forces perpendicular to the field lines and is described by the so-called Grad-Shafranov equation. This is a complicated nonlinear equation for which no general solutions are available. Because of the mathematical difficulties (e.g., Heinemann and Olbert 1978), the analytic studies have been characterized by simplified approaches, including separation of variables (e.g., Tsinganos and Trussoni 1990; Sauty and Tsinganos 1994), self-similarity (e.g., BP; Bacciotti and Chiuderi 1992; Contopoulos and Lovelace 1994; Lynden-Bell and Boily 1994), previously “guessed” magnetic configurations (e.g., Pudritz and Norman 1983; Lery et al. 1998), as well as examinations of various asymptotic limits to the theory (e.g., Heyvaerts and Norman 1989, HN; Appl and Camenzind 1993; Ostriker 1997). Pelletier and Pudritz (1992) constructed non-self-similar models of disk winds including cases where the wind emerges only from a finite portion of the disk.

Self-similarity imposes a specific structure on the underlying disk. In the BP model, all quantities scale as power laws of spherical radius along a given direction. This directly implies that the Alfvén surface is conical and, similarly, that the disk’s scale height  $H(r)$  scales linearly with  $r$ . Furthermore, inasmuch as the problem contains a characteristic speed, namely the Kepler speed in the disk, one infers that  $V_A \propto C_s \propto V_r \propto V_\infty \propto V_K$ , i.e., that the Alfvén, sound, radial inflow, terminal outflow, and Kepler speeds, respectively, are all proportional to one another. The scaling  $C_s \propto V_K$  implies that the disk temperature has the virial scaling  $T \propto r^{-1}$ . The scaling  $V_r \propto V_K$  as well as the  $H(r)$  relation

imply that, for a constant mass accretion rate  $\dot{M}_{\text{acc}} = -2\pi(2H\rho)V_r r$ , the density  $\rho \propto r^{-3/2}$ . Next, the scaling of the disk Alfvén speed  $V_A \propto V_K$  together with the density result imply that the disk poloidal field (and hence also  $B_\phi$ ) scales as  $r^{-5/4}$ . In turn, the mass load  $k_0 \propto r_0^{-3/4}$  and the wind mass loss rate  $\dot{M}_{\text{wind}}(r_0) \propto \ln r_0$ . More general self-similar models may be constructed by making the more realistic assumption that mass is lost from the disk so that the accretion rate is not constant;  $\dot{M}_{\text{acc}}(r) \propto r^{-\mu}$ . Adopting the radial scaling of the disk magnetic field,  $B_0(r) \propto r^{-\nu}$ , one finds that self-similarity imposes the scaling  $\mu = 2(\nu - 1.25)$  (see eq. [17]).

The work of HN and others (see Heyvaerts and Norman, 1997) has shown that in general two types of collimation are possible, depending on the asymptotic behavior of the current intensity  $I = (c/2)rB_\phi \propto r^2\rho\Omega_0$ . If  $I \rightarrow 0$  as  $r \rightarrow \infty$ , then the field lines are space-filling paraboloids, whereas if this limit for the current is finite, then the flow is collimated to cylinders. The character of the flow therefore depends on the boundary conditions at the disk.

Finally, we note that the stability of magnetized jets with toroidal magnetic fields is strongly assisted by the jet's poloidal magnetic field, which acts as a spinal column for the jet (e.g., Appl and Camenzind 1992).

#### IV. NUMERICAL SIMULATIONS OF DISK WINDS

The advent of numerical simulations has finally made it possible to study the rich, time-dependent behavior of MHD disk winds. This allows one to test the stationary theory presented above as well as to search for the conditions that give rise to episodic outflows. These simulations represent perhaps the main advance in the subject since *Protostars and Planets III*. The published simulations generally assume ideal MHD and may be grouped into two classes: 1) *dynamic MHD disks*, in which the structure and evolution of the magnetized disk is also part of the simulation, and 2) *stationary MHD disks*, in which the underlying accretion disk does not change and provides fixed boundary conditions for the outflow problem.

##### A. Dynamic Disks and Winds

The first numerical calculations of disk winds were published by Uchida and Shibata (1985, US), and Shibata and Uchida (1986). These simulations modeled a magnetized disk in sub-Keplerian rotation and showed that a rapid radial collapse develops in which the initially poloidal field threading the disk is wound up due to the differential rotation. The vertical Alfvén speed, being smaller than the free-fall speed, implies that a strong, vertical toroidal field pressure gradient  $\partial B_\phi^2/\partial z$  must rapidly build up. This force results in the transient ejection of coronal material

above and below the disk as the spring uncoils. The work of US was confirmed by Stone and Norman (1994, SN) using their ideal-MHD, ZEUS 2-D code (Stone and Norman 1992).

If the mean magnetic field energy density is less than the thermal pressure in the disk ( $V_A < C_s$ ), then a strong magnetorotational instability will develop (e.g., Balbus and Hawley 1991, BH). In 2-D, this leads to a vigorous, radial, channel flow and rapid outward transport of angular momentum. SN ran a series of ZEUS 2-D simulations for a uniform magnetic field threading a wedge-shaped disk and a surrounding corona (models defined by 4 parameters). Their simulations investigated three cases (see also Bell and Lucek 1995 and Matsumoto et al. 1996): (A) sub-Keplerian rotation, (B) a Kepler disk with strong disk field, and (C) a Kepler disk with a weak field. In Case A, rapid collapse immediately ensues with an expanding, transient outflow appearing in 2.5 orbits (reproducing US). In Case B, the disk is BH-stable, but collapse occurs anyway because of the very strong braking of the disk due to the external MHD torque. In case C one again sees rapid radial collapse of the disk, this time because of a strong BH instability.

The 2-D channel flow does not, however, persist in 3-D: in that case the BH instability develops into a fully turbulent flow and the inflow rate is significantly reduced (see chapter by Stone et al.).

## B. Stationary Disks and Winds

The outflow problem can be clarified by focusing on the more restricted question of how a wind is accelerated and collimated for a prescribed set of fixed boundary conditions on the disk. Keplerian disks in 3-D are stable on many tens of orbital times and this justifies the stationary disk approach: the launch and collimation of jets from their surfaces occurs in only a few inner-disk rotation times. Groups that have taken this route include Ustyugova et al. (1995), Ouyed et al. (1997, OPS), Ouyed and Pudritz (1997a,b, OPI and OPII), Romanova et al. (1997), and Meier et al. (1997). The published simulations differ in their assumed initial conditions, such as the magnetic field distribution on the disk, the plasma  $\beta$  ( $\equiv P_{\text{gas}}/P_{\text{mag}}$ ) above the disk surfaces, the state of the initial disk corona, and the handling of the gravity of the central star. Broadly speaking, all of the existing calculations show that winds from accretion disks can indeed be launched and accelerated, much along the lines suggested by the theory presented in Sec. III. The results differ, however, in the degree to which flow collimation occurs.

Ustyugova et al. (1995) and Romanova et al. (1997) employed a magnetic configuration described by a monopole field centered beneath the disk surface. Nonequilibrium initial conditions as well as a softened gravitational potential were used. Relatively low resolution simulations of flows with  $\beta \gg 1$  (Ustyugova et al.) showed that collimated, non-stationary outflows develop. Similar simulations in the

strong-field ( $\beta < 1$ ) regime (Romanova et al.) resulted in stationary, but uncollimated outflows on these scales.

Simulations by OPS, OPI, and OPII (see Pudritz and Ouyed 1997 for a review) employed the ZEUS 2-D code and studied two different magnetic configurations. The coronal gas was initially taken to be in hydrostatic equilibrium with the central object as well as in pressure balance with the top of the disk. Two initial magnetic configurations were adopted, each chosen so that no Lorentz force is exerted on the hydrostatic corona, i.e., such that  $\mathbf{j} = 0$ . These are the potential field configuration of Cao and Spruit (1994), and a uniform, vertical field that is everywhere parallel to the disk rotation axis. The gravity was unsoftened in these calculations,  $(500 \times 200)$  spatial zones were used, and simulations were run up to  $400t_i$  (where  $t_i$  is the Kepler time for an orbit at the inner edge of the disk,  $r_i$ ). This model is described by 5 parameters set at  $r_i$ : 3 to describe the initial corona (e.g.,  $\beta_i = 1.0$ ), as well as 2 parameters to describe the disk physics (e.g., the injection speed  $V_{inj}$  of the material from the disk into the base of the corona). The initial conditions correspond to turning on the rotation of the underlying Keplerian disk at  $t = 0$ .

The first thing that happens is the launch and propagation of a brief transient, torsional Alfvén wave front that sweeps out from the disk surface but that leaves the corona largely undisturbed. An outflow also begins almost immediately and develops into a stationary or an episodic jet. These jet-like outflows are highly collimated and terminate in a jet shock. A bow shock, driven by the jet, pushes through the corona. A noticeably empty cavity dominates most of the volume behind the bow shock: the cavity is filled by the toroidal magnetic field that is generated by the jet itself. This may provide an explanation of the extended bipolar cavities that surround highly collimated jets. For a fiducial injection speed of  $10^{-3}V_K$ , the potential field configuration developed into a stationary outflow with many (but not all, since the flow is not self-similar) of the characteristics of the BP solution. The Alfvén surface is correctly predicted by the analysis in section III. The Alfvén and fast-magnetosonic Mach numbers reach 5 and 1.6, respectively, at  $z = 10r_i$ , with the toroidal-to-poloidal field-strength ratio being  $\sim 3$  on this scale. Outflow only takes place on field lines that are inclined by less than  $60^\circ$  with respect to the disk surface, as predicted by BP.

Figure 1 (adapted from OPS) shows that the poloidal field lines in the initial state are collimated toward the rotation axis by the hoop stress of the jet's toroidal field. The figure also shows the propagation of the jet-driven bow-shock and the eventual creation of a cylindrically collimated jet with well determined Alfvén and fast-magnetosonic critical surfaces in the acceleration region above the disk (the slow-magnetosonic surface is too close to the disk to be resolved in this figure).

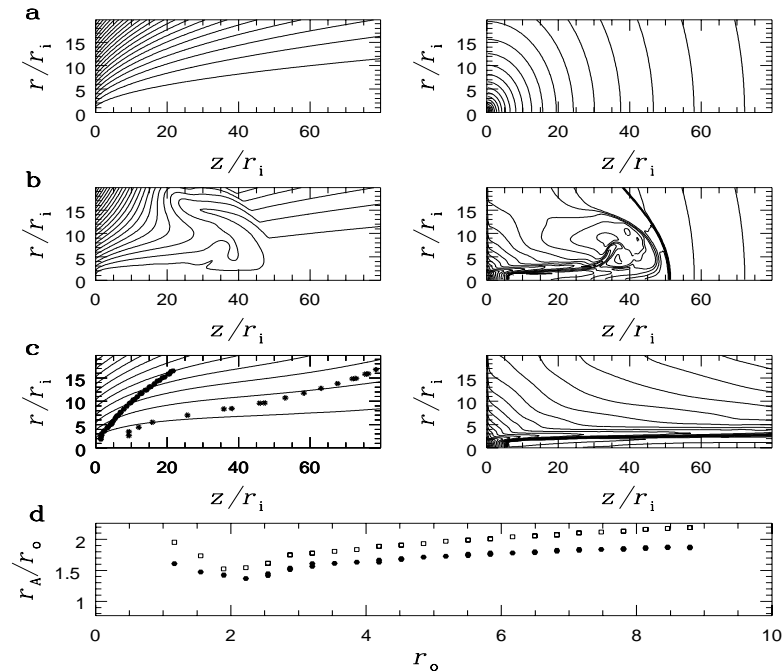


Figure 1. Numerical simulations of disk-driven MHD outflows (adapted from OPS). In frame *a*, the left panel shows the initial magnetic configuration corresponding to the “potential field” solution, whereas the right panel displays the initial isodensity contours of the corona. The flow injection speed is  $V_{\text{inj}} = 10^{-3}V_K$ . Frames *b* and *c* show the evolution of the initial magnetic and density structures (the left and right panels, respectively) at 100 and 400 inner time units. Frame *c* also displays the locations of the Alfvén critical surface (filled hexagons) and the FM surface (stars). In frame *d*, the Alfvén lever arm ( $r_A/r_0$ ) found in the simulation is shown (filled hexagons) as a function of the location ( $r_0$ ) of the footpoints of the field lines on the disk, and is compared to the prediction from the steady-state theory of Sec. III.A (squares).

For the same boundary and initial conditions, the initially vertical field configuration leads to the development of a jet that is episodic over the 400  $t_i$  duration of the simulation (OPS, OPII). Even though the initial configuration is highly unfavorable to jet formation, jet production occurs. The reason for this is the effect of the toroidal field in the corona, which is concentrated towards the inner edge of the disk (where the Kepler rotation is the greatest). It therefore exerts a radial pressure force  $\partial(B_\phi^2/8\pi)/\partial r$  that opens up field lines at larger radii. As long as  $\beta \simeq 1$  in this region, field lines are pliable enough to move,

and a jet is launched. Episodic knots are produced on a time scale  $\tau_{knot} \simeq r_{jet}/V_{A,\phi}$ , which is reminiscent of a type of kink instability. Regions of high toroidal field strength and low density separate and confine the knots, which in turn have high density and low toroidal field strength.

The appearance of stationary or episodic jets has nothing to do with the magnetic configuration, but rather with the mass loading of the magnetic configuration, as is seen in an extensive set of simulations (Ouyed and Pudritz 1998). Figure 2 shows a simulation with the same potential configuration parameters as in Figure 1 except for a reduced injection speed (and hence mass load) of  $V_{inj} = 10^{-5}V_K$ . Clear episodic behavior is now seen in this flow.

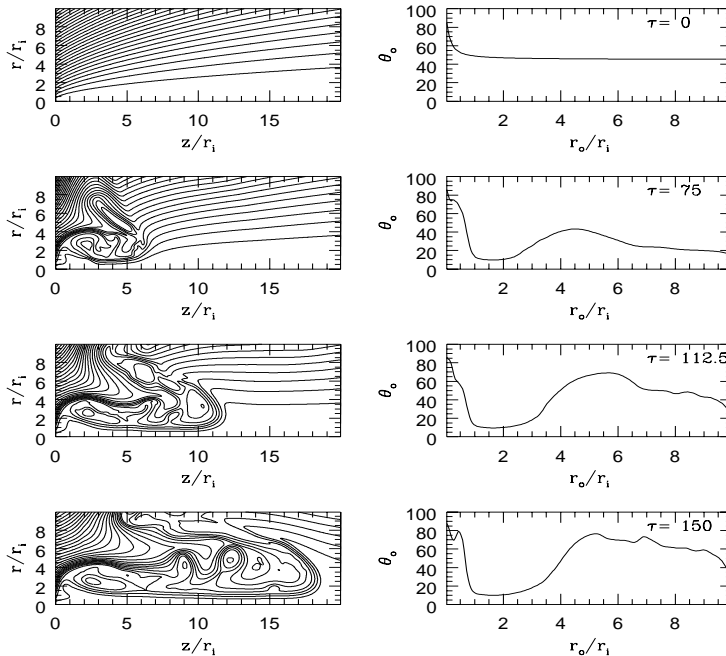


Figure 2. MHD outflow simulations with the same parameters and magnetic configuration as in Fig. 1, except  $V_{inj} = 10^{-5}V_K$  (adapted from Ouyed and Pudritz 1998). The left panels show the magnetic field structure and knot formation at times 0.0, 75.0, 112.5, and 150.0  $t_i$ . The right panels show the angle  $\theta_0$  between the field lines and the disk surface at these 4 times. Only field lines that open up to an angle  $\theta_0 \leq 60^\circ$  are seen to drive an outflow.

Nonsteady outflows could conceivably also arise in highly conducting disk regions where the winding-up of the field lines might eject gas through a strong  $|B_\phi|$  pressure gradient (e.g., Contopoulos 1995).

### C. Far-Field Behavior of MHD Jets

Simulations of MHD jets propagating into a uniform medium show that, in certain respects, they differ dramatically from hydrodynamic jets. Clarke et al. (1986), Lind et al. (1986), and Kössel et al (1990) showed that the strong toroidal field of a jet prevents matter from spraying sideways on encountering the jet shock. Rather, jet material decelerated by a Mach disk and a strong annular shock is focused mainly forward into a nose cone. This contrasts with the backflowing cocoon that characterizes purely hydrodynamic, low-density jets. Hydromagnetic jets are generally preceded by stronger, more oblique shocks and advance far more quickly into the surrounding medium than their hydrodynamic counterparts (see Kössel et al. 1990 for more detail). MHD jets may thus explain why one does not measure strong transverse expansions in bipolar molecular lobes (e.g., Masson and Chernin 1993; Cabrit 1997).

## V. MAGNETIZED PROTOSTELLAR ACCRETION DISKS

### A. Magnetic Angular Momentum Transport

One of the primary reasons why open, ordered magnetic fields are important in accreting astrophysical systems is that they can mediate a vertical transport of angular momentum from accretion disks. In Sec. III we discussed the angular momentum transport by centrifugally driven winds, but it is important to realize that angular momentum can be removed from the disk surfaces even if the field-line inclination with respect to the vertical is not large enough for the wind launching condition to be satisfied, so long as the field is attached to a “load” that exerts a back torque on the disk. In that case the disk can lose angular momentum through torsional Alfvén waves propagating away from the disk surfaces (the “magnetic braking” mechanism; see Mouschovias 1991 for a review). When the magnetic fields are well below equipartition with the gas pressure in a differentially rotating disk, the magnetorotational (Balbus-Hawley) instability develops on a dynamical time scale and produces a magnetic stress-dominated turbulence that gives rise to radial transport of angular momentum characterized by an effective viscosity parameter  $\alpha$  that lies in the range  $\sim 0.005 - 0.5$  (see chapter by Stone et al.).

Numerical simulations (see Sec. IV.A) have demonstrated that all of the above processes could contribute to the angular momentum transport in magnetized disks. One can estimate the relative roles of vertical wind transport and radial turbulent transport by taking the ratio of the external wind torque computed in Sec. III and the viscous torque associated with magnetocentrifugal turbulence, which can be written as  $(B_z^2/4\pi P_{\text{gas}})(r_A/\alpha H)$  (Pelletier and Pudritz 1992). Thus, even if the ordered field threading the disk were far below equipartition



with the disk gas pressure, a wind torque could still dominate a turbulent torque simply because of its large lever arm (the Alfvén radius  $r_A$ , which greatly exceeds the disk scale height  $H$ ). We note in passing that a long effective lever arm also characterizes angular momentum transport by spiral waves in the disk.

The requirement that, in a steady state, the torque exerted by a large-scale magnetic field at the surface of a thin and nearly Keplerian accretion disk balances the inward angular momentum advection rate can be written as  $\dot{M}_{\text{acc}} = 2 r^{5/2} |B_z B_{\phi,s}| / (G M_*)^{1/2}$  (see eq. [17]). Assuming a rough equality between the vertical and azimuthal surface field components, this relation implies that, at a distance of 1 AU from a solar-mass protostar, a 1 G field (the value indicated by meteoritic data for the protosolar nebula; Levy and Sonett 1978) could induce accretion at a rate of  $\sim 2 \times 10^{-6} M_{\odot} \text{ yr}^{-1}$ , which is compatible with the mean values inferred in embedded protostars (see Sec. II.B). For comparison, the minimum-mass solar nebula model implies a thermal pressure at 1 AU that corresponds to an equipartition magnetic field of  $\sim 18$  G, which implies that a  $\sim 1$  G field could be readily anchored in the protosolar disk at that location.

## B. Wind-Driving Protostellar Disk Models

The properties of protostellar accretion disks and of integrated disk/wind systems have, so far, been derived only under highly simplified assumptions. Among the papers that can be consulted on this topic are Königl (1989, 1997), Wardle and Königl (1993), Ferreira and Pelletier (1993a,b, 1995; also Ferreira 1997), Lubow et al. (1994), Li (1995, 1996), and Reyes-Ruiz and Stepinski (1996). A plausible origin for an open disk magnetic field is the interstellar field that had originally threaded the magnetically supported molecular cloud and that was subsequently carried in by the collapsing core. This picture is favored over disk-dynamo interpretations in view of the fact that the latter typically produce closed (quadrupolar) field configurations, although we note that scenarios for opening dynamo-generated field lines have been considered in the literature (e.g., Tout and Pringle 1996; Curry, Pudritz, and Sutherland 1994).

The theory and simulations of the previous sections assumed ideal MHD. While this approximation is adequate for the surface layers of protostellar disks, the disk interiors are typically weakly ionized, and their study entails the application of multifluid MHD. For typical parameters of disks around solar-mass YSOs, one can distinguish between the low-density regime (on scales  $r \lesssim 100$  AU), in which the current in the disk is carried by metal ions and electrons (whose densities are determined from the balance between ionizations by cosmic rays and recombinations on grain surfaces), and the high-density regime (on scales  $r \lesssim 1 - 10$  AU), where the current is carried by small charged grains or

by ions and electrons that recombine without grains. We restrict our attention to the low-density regime and concentrate on the case where the magnetic field  $\mathbf{B}$  is “frozen” into the electrons and diffuses relative to the dominant neutral component as a result of an ion–neutral drift (ambipolar diffusion).

To derive a self-consistent steady-state disk/wind configuration, one combines the mass, momentum (radial, vertical, and angular), and energy conservation relations, together with Maxwell’s equations and the generalized Ohm’s law, and imposes the requirements that the outflow pass through the relevant critical points (see Sec. IV). So far only simple prescriptions for the disk thermal structure (isothermal or adiabatic) and conductivity (ambipolar diffusion in the density regime where the ion density is constant or Ohmic diffusivity parametrized using a “turbulence” prescription) have been considered. These are probably adequate for obtaining the basic structure of the disk, but more realistic calculations are needed to correctly model the transition region between the disk and the wind.

The vertical structure of a generic centrifugal wind-driving disk (or “active” surface layer; see Sec. V.C) can be divided into 3 distinct zones (see Fig. 3): a quasi-hydrostatic region near the midplane of the disk, where the bulk of the matter is concentrated and most of the field-line bending takes place, a transition zone where the inflow gradually diminishes with height, and an outflow region that corresponds to the base of the wind. The first two regions are characterized by a radial inflow and sub-Keplerian rotation, while the gas at the base of the wind flows out with  $V_\phi > V_K$ . The boundary conditions for the stationary disk simulations discussed in Sec. IV.B arise from the physical properties of this latter region.

What determines the disk structure and how does the magnetic field extract the angular momentum of the accreting gas? The quasi-hydrostatic region is matter dominated, with the ionized plasma and magnetic field being carried around by the neutral material. The ions are braked by a magnetic torque, which is transmitted to the neutral gas through the frictional (ambipolar-diffusion) drag; therefore  $V_{i\phi} < V_\phi$  in this region (with the subscript  $i$  denoting ions). The neutrals thus lose angular momentum to the field, and their back reaction leads to a buildup of the azimuthal field component  $|B_\phi|$  away from the midplane. The loss of angular momentum enables the neutrals to drift toward the center, and in doing so they exert a radial drag on the field lines. This drag must be balanced by magnetic tension, so the field lines bend away from the rotation axis. This bending builds up the ratio  $B_r/B_z$ , which needs to exceed  $1/\sqrt{3}$  at the disk surface to launch a centrifugally driven wind. The magnetic tension force, transmitted through ion–neutral collisions, contributes to the radial support of the neutral gas and causes it to rotate at sub-Keplerian speeds.

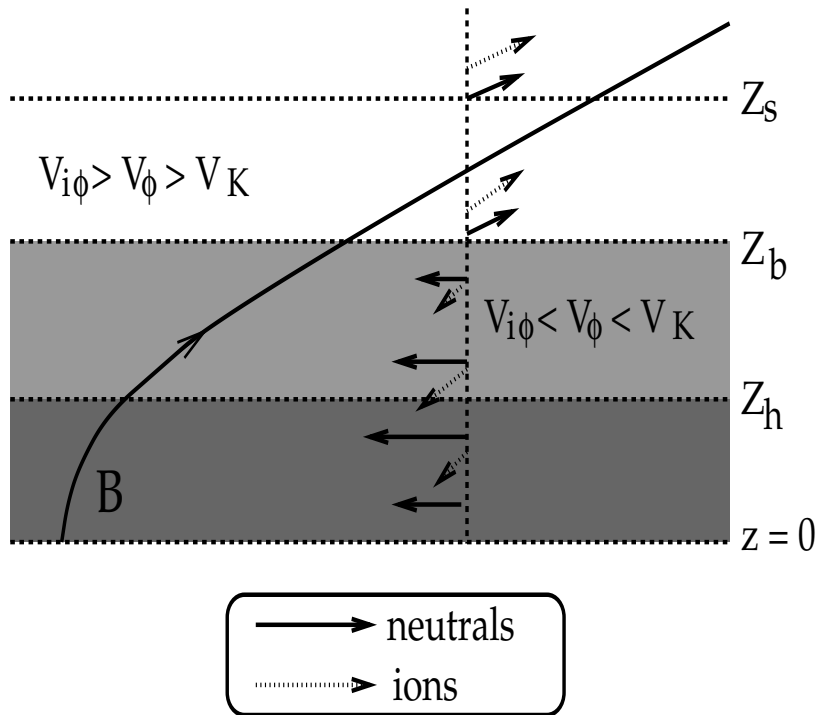


Figure 3. Schematic diagram of the vertical structure of an ambipolar diffusion-dominated disk, showing a representative field line and the poloidal velocities of the neutral (solid arrowheads) and the ionized (open arrowheads) fluid components. Note that the poloidal velocity of the ions vanishes at the midplane ( $z = 0$ ) and is small for both fluids at the base of the wind ( $z = Z_b$ ). The relationship between the azimuthal velocities is also indicated.

The growth of the radial and azimuthal field components on moving away from the midplane results in a magnetic pressure gradient that tends to compress the disk. The vertical compression by the combined magnetic and tidal stresses is, in turn, balanced by the thermal pressure gradient. The magnetic energy density becomes dominant as the gas density decreases, marking the beginning of the transition zone (at  $z = Z_h$ ). The field above this point is nearly force free ( $[\nabla \times \mathbf{B}] \times \mathbf{B} \approx 0$ ), so the field lines, which vary only on a length scale  $\sim r$ , are locally straight. This is the basis for the adoption of force-free initial field configurations in the simulations reviewed in Sec. IV.B.

The field angular velocity, given by  $\omega = (V_{i\phi} - V_{iz}B_\phi/B_z)/r$ , is a field-line constant (corresponding to  $\psi$  in the ideal-MHD case; see Sec. III.A). The ion angular velocity  $V_{i\phi}/r$  differs somewhat from  $\omega$  but still changes only slightly along the field. Since the field lines bend

away from the symmetry axis, the cylindrical radius  $r$ , and hence  $V_{i\phi}$ , increase along any particular field line, whereas  $V_\phi$  decreases because of the near-Keplerian rotation law. Eventually a point is reached where  $(V_{i\phi} - V_\phi)$  changes sign. At this point, the magnetic stresses on the neutral gas are small and its angular velocity is almost exactly Keplerian. Above this point, the field lines overtake the neutrals and transfer angular momentum back to the matter, and the ions start to push the neutrals out in both the radial and the vertical directions. It is thus natural to identify the base  $Z_b$  of the wind with the location where the angular velocity of the field lines becomes equal to the Keplerian angular velocity. The mass outflow rate is fixed by the height  $Z_s$  of the effective sonic point of the wind.

As was first recognized by Wardle and Königl (1993), one can derive key constraints on a viable solution by neglecting the vertical component of the neutral velocity, which is generally a good approximation throughout much of the disk column. This simplifies the problem by transforming the radial and azimuthal components of the neutral momentum equation into algebraic relations. One important constraint that can be derived in this way expresses the intuitively obvious condition that the neutrals must be able to couple to the magnetic field on an orbital time scale if magnetic torques are to play a role in the removal of angular momentum from the disk. In the pure-ambipolar-diffusion regime, this condition is expressed by the requirement that the neutral-ion coupling time  $1/\gamma\rho_i$  (where  $\gamma \approx 3.5 \times 10^{13} \text{ cm}^3 \text{ g}^{-1} \text{ s}^{-1}$  is the collisional coupling coefficient) be shorter than the dynamical time. This is equivalent to requiring that the neutral-ion coupling parameter  $\eta \equiv \gamma\rho_i r/V_K$  satisfy

$$\eta > 1. \quad (20)$$

This condition is quite general and is relevant also to disk models in which magnetic torques associated with small-scale magnetic fields transfer angular momentum radially through the disk (see chapter by Stone et al.; in the latter case eq. [20] identifies the linearly unstable regime of the magnetorotational instability, although evidently a much higher minimum value of  $\eta$  is required for significant nonlinear growth).

Additional parameter constraints that can be derived by using the hydrostatic approximation for a wind-driving disk model in the pure-ambipolar-diffusion regime are given by

$$(2\eta)^{-1/2} \lesssim a \lesssim 2 \lesssim \epsilon\eta \lesssim V_K/2C_s, \quad (21)$$

where  $a \equiv B_0/(4\pi\rho_0)^{1/2}C_s$  is the ratio of the midplane (subscript 0) Alfvén speed to the isothermal sound speed  $C_s$  and  $\epsilon \equiv -V_{r0}/C_s$  is the normalized midplane inflow speed. The first inequality corresponds to the requirement that the disk remain sub-Keplerian, the

second to the wind-launching condition at the disk surface (subscript  $b$ )  $B_r(Z_b) \gtrsim B_0/\sqrt{3}$ , and the third to the requirement that the base of the wind lie well above a density scale height in the disk. The second and third inequalities together imply that the vertical magnetic stress dominates the gravitational tidal stress in confining the disk: this is a generic property of this class of disk solutions that does not depend on the nature of the magnetic diffusivity. The last inequality expresses the requirement that the ambipolar diffusion heating rate at the midplane not exceed the rate  $\rho_0|V_{r0}|V_k/2r$  of gravitational potential energy release. In turn,  $C_s/V_K$  must be  $\ll 1/(1+\epsilon)$  to guarantee that the disk is in near-Keplerian motion and geometrically thin. One can also place upper limits on the density at the sonic point to ensure that the bulk of the disk material is hydrostatic and that  $\dot{M}_{\text{wind}}$  does not exceed  $\dot{M}_{\text{acc}}$ . Similar constraints are derived by applying this analysis to the other diffusivity regimes identified above. The solutions that satisfy these constraints tend to have  $\epsilon \lesssim 1$  and  $a \gtrsim 1$ . Furthermore, the magnetic field in these models, whose magnitude is essentially determined from the condition that all the angular momentum liberated by the accreting matter is transported by a centrifugally driven wind, automatically lies in a “stability window” where it is strong enough not to be affected by the magnetorotational instability but not so strong as to be subject to the radial interchange instability (Königl and Wardle 1996).

As we have noted, the steady-state disk models are useful for guiding the choice of boundary conditions at the base of the outflow in numerical simulations of winds from quasi-stationary disks. In a complementary approach (which typically employs a highly simplified treatment of the disk outflow and therefore is not suitable for a detailed study of the disk wind), one can generalize the steady-state models and investigate the time evolution of wind-driving accretion disks (e.g. Lovelace et al. 1994; Königl 1997). The time-dependent models can be utilized to explore the feedback effect between the magnetic flux distribution, which affects the angular momentum transport in the disk, and the radial inflow induced by the magnetic removal of angular momentum, which can modify the flux distribution through field-line advection.

### C. Outflows from the Protostellar Vicinity

As one moves to within a few AU from the protostar, the disk hydrogen column density can become so large ( $\gtrsim 192 \text{ g cm}^{-2}$ ) that cosmic rays are excluded from the disk interior. (For reference, the column density of the minimum-mass solar nebula model is  $1.7 \times 10^3 \text{ g cm}^{-2}$  at 1 AU). At larger columns the ionization rate is dominated by the decay of radioactive elements (notably  $^{26}\text{Al}$  if it is present and  $^{40}\text{K}$ ; Stepinski 1992), but the charge density generally becomes too low for the magnetic field to be effectively coupled to the matter. Consequently, the

interior of the disk becomes inert and magnetically mediated accretion can only proceed through “active” surface layers that extend to a depth of  $\sim 96 \text{ g cm}^{-2}$  on each side of the disk. This scenario applies both to a wind-driving disk (Wardle 1997) and to the case where small-scale magnetic fields produce an effective viscosity within the disk (Gammie 1996). Galactic cosmic rays could reach the disk along the open magnetic field lines that thread it, but a super-Alfvénic outflow along these field lines would tend to exclude them. External ionization could, however, also be effected by stellar X-rays (see chapter by Glassgold et al.) as well as by fast particles accelerated in stellar flares. In addition, heating by stellar irradiation could contribute to the collisional ionization of the surface layers (e.g., D’Alessio et al. 1998).

The entire disk can recover an adequate coupling with the magnetic field once the central temperature becomes large enough for collisional ionization to be effective. This first occurs when the temperature increases above  $\sim 10^3 \text{ K}$  and potassium is rapidly ionized (e.g., Umebayashi and Nakano 1981). For disks in which magnetic fields dominate the angular momentum transport, it may be possible that Joule dissipation could maintain the requisite degree of ionization for efficient gas–field coupling ( $\eta > 1$ ; see eq. [20]). Li (1996) first explored this possibility for the inner regions of wind-driving protostellar disks and concluded that, for a disk that is in the ambipolar-diffusion regime on scales  $\lesssim 1 \text{ AU}$ , a self-consistent model can only be constructed if the accretion rate is very high ( $\gtrsim 10^{-5} M_{\odot} \text{ yr}^{-1}$ ).

A possible mechanism for recoupling the gas to the field in the vicinity of the YSO is the thermal ionization instability originally discussed in the context of dwarf novae and more recently invoked as a possible explanation of FU Orionis outbursts (e.g., Bell & Lin 1994). In this picture, accretion in the innermost disk proceeds in a nonsteady fashion, with a “gate” at  $r \lesssim 0.25 \text{ AU}$  opening every  $\sim 10^3 \text{ yr}$  or so after the accumulated column density has become large enough to trigger the instability. During the “high” phase of the instability (which lasts  $\sim 10^2 \text{ yr}$  and is identified with an outburst) the gas is hot ( $T \gtrsim 10^4 \text{ K}$ ) and almost completely ionized, and mass rains in at a rate  $\sim (1 - 30) \times 10^{-5} M_{\odot} \text{ yr}^{-1}$ , whereas during the “low” phase the temperature and degree of ionization decline sharply, and the accretion rate drops to  $\sim (1 - 30) \times 10^{-8} M_{\odot} \text{ yr}^{-1}$ . In the context of the magnetized disk model, one can attribute the increase in the accretion rate as the gas becomes highly ionized to the reestablishment of good coupling between the field and the matter, which allows the field to extract the angular momentum of the accreting gas. This could account both for the marked increase in  $\dot{M}_{\text{acc}}$  and for the strong disk outflow that accompanies it (see Sec. II.B). The magnetic recoupling idea may be relevant to these outbursts even if the wind is not the dominant angular momentum transport mechanism in the disk provided that the

viscosity has a magnetic origin (see chapter by Stone et al.). We note, however, that the relatively large ( $\sim 0.1$ )  $\dot{M}_{\text{wind}}/\dot{M}_{\text{acc}}$  ratio indicated in some of the outburst sources is consistent with the bulk of the disk angular momentum being removed by the wind.

At distances of a few stellar radii, the stellar magnetic field could be strong enough to drive outflows from the disk. Various scenarios have been considered in this connection, including individual magnetic loops ejecting diamagnetic blobs through a magnetic surface drag force (King and Regev 1994); a steady-state configuration in which mass is transferred to the star near the corotation radius and an outflow is driven along adjacent (but disconnected from the star) field lines (Shu et al. 1994), and time-dependent ejection associated with the twisting, expansion, and subsequent reconnection of field lines that connect the star with the disk (Hayashi et al. 1996; Goodson et al. 1997). Numerical simulations are rapidly reaching the stage where they could be utilized to identify the relevant mechanisms and settle many of the outstanding questions. There are already indications from some of the existing simulations that magnetically channeled accretion from the disk to the star is most likely to occur when the disk carries a strong axial magnetic field that reconnects with the stellar field at an equatorial X-point; the resulting field configuration appears to be quasi-steady and gives rise to sturdy centrifugally driven outflows along open field lines (Hirose et al. 1997; Miller and Stone 1997).

Stellar field-driven outflows are the subject of the chapter by Shu et al. This class of models is based on the realization that stellar magnetic field lines can be inflated and opened up through an interaction with a surrounding disk, and that a centrifugal wind can be driven out along the opened field lines. In these scenarios, the outflow typically originates near the inner disk radius, where the disk is truncated by the stellar magnetic stresses. This contrasts with the scenarios considered in this chapter, wherein a disk-driven wind originates (and can contribute to the disk angular momentum transport) over a significant range of radii. It is worth noting in this connection that the massive inflows that characterize FU Orionis outbursts are expected to crush the respective stellar magnetospheres, so the strong outflows that are inferred to originate from the circumstellar disks during these outbursts are unlikely to be driven along stellar field lines (Hartmann and Kenyon 1996). Coupled with the apparent inadequacy of thermal-pressure and radiative driving, this argument provides strong support for the relevance of disk-driven hydromagnetic winds that are not associated with a stellar magnetic field to the observed outflows from FU Orionis outburst sources. The ramifications of this argument become even stronger if a significant fraction of the mass accumulation in solar-type stars occurs through such outbursts during the early phases of their evolution (Hartmann 1997). To be sure, the “distributed” disk-wind models dis-

cussed in this chapter are meant to apply to YSOs in general and not just when they undergo an outburst, but only during an FU Orionis outburst does the disk become sufficiently luminous that an unambiguous observational signature of an extended disk wind can be obtained.

## VI. CONCLUSIONS

Centrifugally driven winds from disks threaded by open magnetic field lines provide the most efficient way of tapping the gravitational potential energy liberated in the accretion process to power an outflow. The fact that such winds “automatically” carry away angular momentum and thus facilitate (and possibly even control) the accretion process makes them an attractive explanation for the ubiquity of jets in YSOs and in a variety of other accreting astronomical objects. One of the key findings of recent numerical simulations of MHD winds from disks is that such outflows are indeed easy to produce and maintain under a variety of surface boundary conditions. These simulations have also verified the ability of such outflows to self-collimate and give rise to narrow jets, as well as a variety of other characteristics that are consistent with YSO observations. In the case of protostellar disks, the presence of open field lines is a natural consequence of their formation from the collapse of magnetically supported molecular cloud cores. Although a stellar magnetic field that threads the disk could in principle also play a similar role, this possibility is unlikely to apply to the strong outflows associated with FU Orionis outbursts. (More generally, it is worth noting that, in contrast to disk field-driven outflows, a scenario that invokes a stellar field may not represent a universal mechanism since many cosmic jet sources are associated with a black hole that does not provide an anchor for a central magnetic field.) Much progress has also been achieved in constructing global MHD disk/wind models, but the full elucidation of this picture and its consequences for star formation remains a challenge for the future.

*Acknowledgments.* We thank Vincent Mannings, Rachid Ouyed, and the anonymous referee for helpful comments on the manuscript. This work was supported in part by NASA grant NAG 5-3687 (A.K.) and by an operating grant from the Natural Science and Engineering Research Council of Canada (R.P.).



## REFERENCES

- Appl, S., and Camenzind, M. 1992. The stability of current carrying jets. *Astron. Astrophys.* 256:354–370.
- Appl, S., and Camenzind, M. 1993. The structure of MHD jets: a solution to the non-linear Grad-Shafranov equation. *Astron. Astrophys.* 274:699–706.
- Bacciotti, F., and Chiuderi, C. 1992. Axisymmetric magnetohydrodynamic equations: exact solutions for stationary incompressible flows. *Phys. Fluids B* 4:35–43.
- Balbus, S. A., and Hawley, J. F. 1991. A powerful local shear instability in weakly magnetized disks. I - Linear analysis. II - Nonlinear evolution. *Astrophys. J.* 376, 214–233.
- Bell, K. R. 1994. Reconciling accretion scenarios with inner holes: the thermal instability and the  $2\mu\text{m}$  gap. In *ASP Conf. Ser. 62, The Nature and Evolution of Herbig Ae/Be Stars*, eds. P. S. Thé, M. R. Pérez, and E. P. J. van den Heuvel (San Francisco: ASP), pp. 215–218.
- Bell, K. R., and Lin, D. N. C. 1994. Using FU Orionis outbursts to constrain self-regulated protostellar disk models. *Astrophys. J.* 427:987–1004.
- Bell, A. R., and Lucek, S. G. 1995. Magnetohydrodynamic jet formation. *Mon. Not. Roy. Astron. Soc.* 277:1327–1340.
- Blandford, R. D., and Payne, D. G. 1982. Hydromagnetic flows from accretion discs and the production of radio jets. *Mon. Not. Roy. Astron. Soc.* 199:883–903.
- Bontemps, S., André, P., Terebey, S., and Cabrit, S. 1996. Evolution of outflow activity around low-mass embedded young stellar objects. *Astron. Astrophys.* 311:858–872.
- Burrows, C. J., et al. 1996. Hubble Space Telescope observations of the disk and jet of HH 30. *Astrophys. J.* 473:437–451.
- Cabrit, S., and André, P. 1991. An observational connection between circumstellar disk mass and molecular outflows. *Astrophys. J.* 379:L25-L28.
- Cabrit, S., Edwards, S., Strom, S. E., and Strom, K. M. 1990. Forbidden line emission and infrared excesses in T Tauri stars - Evidence for accretion-driven mass loss? *Astrophys. J.* 354:687–700.
- Cabrit, S., Raga, A. C., and Gueth, F. 1997. Models of bipolar molecular outflows. In *Herbig-Haro Flows and the Birth of Low Mass Stars*, eds. B. Reipurth and C. Bertout (Dordrecht: Kluwer), pp.

- 163–180.
- Calvet, N., Hartmann, L., and Kenyon, S. J. 1993. Mass loss from pre-main-sequence accretion disks. I. The accelerating wind of FU Orionis. *Astrophys. J.* 402:623–634.
- Cao, X., and Spruit, H. C. 1994. Magnetically driven wind from an accretion disk with low-inclination field lines. *Astron. Astrophys.* 287:80–86.
- Ciolek, G. E., and Königl, A. 1998. Dynamical collapse of nonrotating magnetic molecular cloud cores: evolution through point-mass formation. *Astrophys. J.* 504:257–.
- Clarke, D. A., Norman, M. L., and Burns, J. O. 1986. Numerical simulations of a magnetically confined jet. *Astrophys. J.* 311:L63–L67.
- Contopoulos, J. 1995. A simple type of magnetically driven jets: An astrophysical plasma gun. *Astrophys. J.* 450:616–627.
- Contopoulos, J., and Lovelace, R. V. E. 1994. Magnetically driven jets and winds: exact solutions. *Astrophys. J.* 429:139–152.
- Corcoran, M., and Ray, T. 1997. Forbidden emission lines in Herbig Ae/Be stars. *Astron. Astrophys.* 321:189–201.
- Corcoran, M., and Ray, T. 1998. Wind diagnostics and correlations with the near-infrared excess in Herbig Ae/Be stars. *Astron. Astrophys.* 331:147–161.
- Crutcher, R. M., Mouschovias, T. Ch., Troland, T. H., and Ciolek, G. E. 1994. Structure and evolution of magnetically supported molecular clouds: evidence for ambipolar diffusion in the Barnard 1 cloud. *Astrophys. J.* 427:839–847.
- Crutcher, R. M., Roberts, D. A., Mehringer, D. M., and Troland, T. H. 1996. HI Zeeman measurements of the magnetic field in Sagittarius B2. *Astrophys. J.* 462:L79–82.
- Crutcher, R. M., Troland, T. H., Goodman, A. A., Heiles, C., Kazés, I., and Myers, P. C. 1993. OH Zeeman observations of dark clouds. *Astrophys. J.* 407:175–184.
- Curry, C., Pudritz, R. E., and Sutherland, P. G. 1994. On the global stability of magnetized accretion disks. I. Axisymmetric modes. *Astrophys. J.* 434:206–220.
- D’Alessio, P., Cantó, J., Calvet, N., and Lizano, S. 1998. Accretion disks around young objects. I. The detailed vertical structure. *Astrophys. J.* 500:411–427.
- Eisloffel, J., and Mundt, R. 1997. Parsec-scale jets from young stars. *Astron. J.* 114:280–287.
- Ferreira, J. 1997. Magnetically-driven jets from Keplerian accretion discs. *Astron. Astrophys.* 319:340–359.
- Ferreira, J., and Pelletier, G. 1993a. Magnetized accretion-ejection structures. I. General statements. *Astron. Astrophys.* 276:625–636.

- Ferreira, J., and Pelletier, G. 1993b. Magnetized accretion-ejection structures. II. Magnetic channeling around compact objects. *Astron. Astrophys.* 276:637–647.
- Ferreira, J., and Pelletier, G. 1995. Magnetized accretion-ejection structures. III. Stellar and extragalactic jets as weakly dissipative disk outflows. *Astron. Astrophys.* 295:807–832.
- Gammie, C. F. 1996. Layered Accretion in T Tauri Disks. *Astrophys. J.* 457:355–362.
- Gomez, M., Whitney, B. A., and Kenyon, S. J. 1997. A survey of optical and near-infrared jets in taurus embedded sources. *Astron. J.* 114:1138–1153.
- Goodson, A. P., Winglee, R. M., and Böhm, K.-H. 1997. Time-dependent accretion by magnetic young stellar objects as a launching mechanism for stellar jets. *Astrophys. J.* 489:199–209.
- Greaves, S., and Holland, W. S. 1998. Twisted magnetic field lines around protostars. *Astron. Astrophys.* 333:L23–L26.
- Greaves, J. S., Holland, W. S., and Murray, A. G. 1995. Magnetic field compression in the Mon R2 cloud core. *Mon. Not. Roy. Astron. Soc.* 297:L49–L52.
- Greaves, J. S., Murray, A. G., and Holland, W. S. 1994. Investigating the magnetic field structure around star formation cores. *Mon. Not. Roy. Astron. Soc.* 284:L19–L22.
- Hartigan, P., Edwards, S., and Ghandour, L. 1995. Disk accretion and mass loss from young stars. *Astrophys. J.* 452:736–768.
- Hartigan, P., Morse, J., and Raymond, J. 1994. Mass-loss rates, ionization fractions, shock velocities, and magnetic fields of stellar jets. *Astrophys. J.* 136:124–143.
- Hartmann, L. 1997. The observational evidence for accretion. In *Herbig-Haro Flows and the Birth of Low Mass Stars*, eds. B. Reipurth and C. Bertout (Dordrecht: Kluwer), pp. 391–405.
- Hartmann, L., and Calvet, N. 1995. Observational constraints on Fu Ori winds. *Astron. J.* 109:1846–1855.
- Hartmann, L., and Kenyon, S. J. 1996. The FU Orionis Phenomenon. *Ann. Rev. Astron. Astrophys.* 34:207–240.
- Hartmann, L., Kenyon, S. J. and Calvet, N. 1993. The excess infrared emission of Herbig Ae/Be stars: disks or envelopes? *Astrophys. J.* 407:219–231.
- Hayashi, M. R., Shibata, K., and Matsumoto, R. 1996. X-ray flares and mass outflows driven by magnetic interaction between a protostar and its surrounding disk. *Astrophys. J.* 468:L37–L40.
- Heinemann, M., and Olbert, S. 1978. Axisymmetric ideal MHD stellar wind flow. *J. Geophys. Res.* 83:2457–2460.
- Heyvaerts, J., and Norman, C. A. 1989. The collimation of magnetized winds. *Astrophys. J.* 347:1055–1081.
- Heyvaerts, J., and Norman, C. A. 1997. In *IAU Symposium 182*,

- Herbig-Haro Flows and the Birth of Low Mass Stars*, eds. B. Reipurth, and C. Bertout (Dordrecht: Kluwer), pp. 275–290.
- Hildebrand, R. H., Dotson, J. L., Dowell, C. D., Platt, S. R., Schleuning, D., Davidson, J. A., and Novak, G. 1995. Far-infrared polarimetry. In *ASP Conf. Ser. 73, Airborne Astronomy Symposium on the Galactic Ecosystem*, eds. M. R. Haas, J. A. Davidson, and E. F. Erickson (San Francisco: ASP), pp. 97–104.
- Hillenbrand, L. A., Strom, S. E., Vrba, F. J., and Keene, J. 1992. Herbig Ae/Be stars - Intermediate-mass stars surrounded by massive circumstellar accretion disks. *Astrophys. J.* 397:613-643.
- Hirose, S., Uchida, Y., Shibata, K., and Matsumoto, R. 1997. *Publ. Astron. Soc. Japan* 49:193–205.
- King, A. R., and Regev, O. 1994. Spin rates and mass loss in accreting T Tauri stars. *Mon. Not. Roy. Astron. Soc.* 268:L69–L73.
- Königl, A. 1989. Self-similar models of magnetized accretion disks. *Astrophys. J.* 342:208–223.
- Königl, A. 1997. Magnetized accretion disks and the origin of bipolar outflows. In *ASP Conf. Ser. 121, Accretion phenomena and related outflows*, eds. D. T. Wickramasinghe, G. V. Bicknell, and L. Ferrario (San Francisco: ASP), pp. 551–560.
- Königl, A. 1999. Theory of bipolar outflows from high-mass young stellar objects. *New Astron. Rev.*, in press.
- Königl, A., and Ruden, S. P. 1993. Origin of outflows and winds. In *Protostars & Planets III*, eds. E. H. Levy and J. I. Lunine (Tucson: Univ. of Arizona Press), pp. 641–688.
- Königl, A., and Wardle, M. 1996. A comment on the stability of magnetic wind-driving accretion discs. *Mon. Not. Roy. Astron. Soc.* 279:L61–L64.
- Kössel, D., Müller, E., and Hillebrandt, W. 1990. Numerical simulations of axially symmetric magnetized jets. *Astron. Astrophys.* 229:401–415.
- Lada, C. J. 1985. Cold outflows, energetic winds, and enigmatic jets around young stellar objects. *Ann. Rev. Astron. Astrophys.* 23:267–317.
- Lery, T., Heyvaerts, J., Appl, S., and Norman, C. A. 1998. Outflows from magnetic rotators. I. Inner structure. *Astron. Astrophys.* 337:603–624.
- Levreault, R. M. 1988. Molecular outflows and mass loss in the pre-main-sequence stars. *Astrophys. J.* 330:897–910.
- Levy, E. H., and Sonnett, C. P. 1978. Meteorite magnetism and early solar system magnetic fields. In *Protostars & Planets*, ed. T. Gehrels (Tucson: Univ. of Arizona Press), pp. 516–532.
- Li, Z.-Y. 1995. Magnetohydrodynamic disk-wind connection: self-similar solutions. *Astrophys. J.* 444:848–860.
- Li, Z.-Y. 1996. Magnetohydrodynamic disk-wind connection: magne-

- to centrifugal winds from ambipolar diffusion-dominated accretion disks. *Astrophys. J.* 465:855–868.
- Lind, K. R., Payne, D. G., Meier, D. L., and Blandford, R. D. 1989. Numerical simulations of magnetized jets. *Astrophys. J.* 344:89–103.
- Lovelace, R. V. E., Romanova, M. M., and Newman, W. I. 1994. Implosive accretion and outbursts of active galactic nuclei. *Astrophys. J.* 437:136–143.
- Lubow, S. H., Papaloizou, J. C. B., and Pringle, J. 1994. Magnetic field dragging in accretion discs. *Mon. Not. Roy. Astron. Soc.* 267:235–240.
- Lynden-Bell, D., and Boily, C. 1994. Self-similar solutions up to flash-point in highly wound magnetostatics. *Mon. Not. Roy. Astron. Soc.* 267:146–152.
- Masson, C. R., and Chernin, L. M. 1993. Properties of jet-driven molecular outflows. *Astrophys. J.* 414:230–241.
- Matsumoto, R., Uchida, Y., Hirose, S., Shibata, K., Hayashi, M. R., Ferrari, A., Bodo, G., and Norman, C. 1996. Radio jets and the formation of active galaxies: accretion avalanches on the torus by the effect of a large-scale magnetic field. *Astrophys. J.* 461:115–126.
- McKee, C. F., Zweibel, E. G., Goodman, A. A., and Heiles, C. 1993. Magnetic fields in star-forming regions: theory. In *Protostars & Planets III*, eds. E. H. Levy and J. I. Lunine (Tucson: Univ. of Arizona Press), pp. 327–366.
- Meier, D., Edgington, S., Godon, P., Payne, D., and Lind, K. 1997. A magnetic switch that determines the speed of astrophysical jets. *Nature* 388:350–352.
- Mestel, L. 1968. Magnetic braking by a stellar wind. *Mon. Not. Roy. Astron. Soc.* 138:359–391.
- Michel, F. C. 1969. Relativistic stellar-wind torques. *Astrophys. J.* 158:727–738.
- Miller, K. A., and Stone, J. M. 1997. Magnetohydrodynamic simulations of stellar magnetosphere–accretion disk interaction. *Astrophys. J.* 489:890–902.
- Miroshnichenko, A., Ivezić, Ž., and Elitzur, M. 1997. On protostellar disks in Herbig Ae/Be stars. *Astrophys. J.* 475:L41–L44.
- Mouschovias, T. Ch. 1991. Cosmic magnetism and the basic physics of the early stages of star formation. In *The Physics of Star Formation and Early Stellar Evolution*, eds. C. J. Lada and N. D. Kylafis (Dordrecht: Kluwer), pp. 61–122.
- Mundt, R., and Ray, T. M. 1994. Optical outflows from Herbig Ae/Be stars and other high luminosity young stellar objects. In *ASP Conf. Ser. 62, The Nature and Evolution of Herbig Ae/Be Stars*, eds. P. S. Thé, M. R. Pérez, and E. P. J. van den Heuvel (San Francisco: ASP), pp. 237–252.

- Ogilvie, G. I., and Livio, M. 1998. On the difficulty of launching an outflow from an accretion disk. *Astrophys. J.* 499:329–339.
- Ostriker, E. 1998. Self-similar magnetocentrifugal disk winds with cylindrical asymptotics. *Astrophys. J.* 486:291–306.
- Ouyed, R., and Pudritz, R. E. 1997. Numerical simulations of astrophysical jets from Keplerian accretion disks. I. Stationary models. *Astrophys. J.* 482:712–732.
- Ouyed, R., and Pudritz, R. E. 1997. Numerical simulations of astrophysical jets from Keplerian accretion disks. II. Episodic outflows. *Astrophys. J.* 484:794–809.
- Ouyed, R., and Pudritz, R. E. 1998. Numerical simulations of astrophysical jets from Keplerian accretion disks. III The effects of mass loading. *Mon. Not. Roy. Astron. Soc.* in press.
- Ouyed, R., Pudritz, R. E., and Stone, J. M. 1997. Episodic jets from black holes and protostars. *Nature* 385:409–414.
- Pelletier, G., and Pudritz, R. E. 1992. Hydromagnetic disk winds in young stellar objects and active galactic nuclei. *Astrophys. J.* 394:117–138.
- Pezzuto, S., Strafella, F., and Lorenzetti, D. 1997. On the circumstellar matter distribution around Herbig Ae/Be stars. *Astrophys. J.* 485:290–307.
- Pudritz, R. E., and Norman, C. A. 1983. Centrifugally driven winds from contracting molecular disks. *Astrophys. J.* 274:677–697.
- Pudritz, R. E., and Ouyed, R. 1997. Numerical simulations of jets from accretion disks. In *IAU Symposium 182: Herbig-Haro Flows and the Birth of Low Mass Stars*, eds. B. Reipurth, and C. Bertout (Dordrecht: Kluwer), pp. 259–274.
- Pudritz, R. E., Pelletier, G., and Gomez de Castro, A. I. 1991. The physics of disk winds. In *The Physics of Star Formation and Early Stellar Evolution*, eds. C. J. Lada and N. D. Kylafis (Dordrecht: Kluwer), pp. 539–564.
- Pudritz, R. E., Wilson, C. D., Carlstrom, J. E., Lay, O. P., Hills, R. E., and Ward-Thompson, D. 1996. Accretion disks around Class 0 protostars: the case of VLA 1623. *Astrophys. J.* 470:L123–L126.
- Ray, T., Muxlow, T. W. B., Axon, D. J., Brown, A., Corcoran, D., Dyson, J., and Mundt, R. 1997. Large-scale magnetic fields in the outflow from the young stellar object T Tauri S. *Nature* 385:415–417.
- Reipurth, B. 1991. Observations of Herbig-Haro objects. In *Low Mass Star Formation and Pre-Main Sequence Objects*, ed. B. Reipurth (Munich: ESO), pp. 247–279.
- Reyes-Ruiz, M., and Stepinski, T. F. 1996. Axisymmetric two-dimensional computation of magnetic field dragging in accretion disks. *Astrophys. J.* 459:653–665.
- Romanova, M. M., Ustyugova, G. V., Koldoba, A. V., Chechetkin, V.

- M., and Lovelace, R. V. E. 1997. Formation of stationary magnetohydrodynamic outflows from a disk by time-dependent simulations. *Astrophys. J.* 482:708–711.
- Sauty, C., and Tsinganos, K. 1994. Nonradial and nonpolytropic astrophysical outflows III. A criterion for the transition from jets to winds. *Astron. Astrophys.* 287:893–926.
- Schatzman, E. 1962. A theory of the role of magnetic activity during star formation. *Ann. Astrophys.* 25:18–29.
- Schleuning, D. A. 1998. Far-infrared and submillimeter polarization of OMC-1: evidence for magnetically regulated star formation. *Astrophys. J.* 493:811–825.
- Shibata, K., and Uchida, Y. 1986. A magnetohydrodynamical mechanism for the formation of astrophysical jets. II - Dynamical processes in the accretion of magnetized mass in rotation. *Publ. Astron. Soc. Japan* 38:631–660.
- Shu, F. H., Najita, J., Ostriker, E., Wilkin, F., Ruden, S., and Lizano, S. 1994. Magnetocentrifugally driven flows from young stars and disks. I. A generalized model. *Astrophys. J.* 429:781–796.
- Skinner, S. L., Brown, A., and Stewart, R. T. 1993. A high-sensitivity survey of radio continuum emission from Herbig Ae/Be stars. *Astrophys. J. Suppl.* 87:217–265.
- Spruit, H. C. 1996. Magnetohydrodynamic jets and winds from accretion disks. In *NATO ASI Ser. C. 477, Evolutionary processes in binary stars.* eds. R. A. M. J. Wijers, M. B. Davies, and C. A. Tout (Dordrecht: Kluwer), pp. 249–286.
- Stepinski, T. F. 1992. Generation of dynamo magnetic fields in the primordial solar nebula. *Icarus* 97:130–141.
- Stone, J. M., and Norman, M. L. 1992. ZEUS-2D: a radiation magnetohydrodynamics code for astrophysical flows in two space dimensions. II. The magnetohydrodynamic algorithms and tests. *Astrophys. J. Suppl.* 80:791–818.
- Stone, J. M., and Norman, M. L. 1994. Numerical simulations of magnetic accretion disks. *Astrophys. J.* 433:746–756.
- Tout, C. A., and Pringle, J. E. 1996. Can a disc dynamo generate large-scale magnetic fields? *Mon. Not. Roy. Astron. Soc.* 281:219–225.
- Tsinganos, K., and Trussoni, E. 1990. Analytic studies of collimated winds I. Topologies of 2-D helicoidal hydrodynamic solutions. *Astron. Astrophys.* 231:270–276.
- Uchida, Y., and Shibata, K. 1985. A magnetohydrodynamic mechanism for the formation of astrophysical jets. I - Dynamical effects of the relaxation of nonlinear magnetic twists. *Publ. Astron. Soc. Japan* 37:31–46.
- Umebayashi, T., and Nakano, T. 1981. Fluxes of energetic particles and the ionization rate in very dense interstellar clouds. *Publ. Astron.*

- Soc. Japan* 33:617–635.
- Ustyugova, G. V., Koldoba, A. V., Romanova, M. M., Chechetkin, V. M., and Lovelace, R. V. E. 1995. Magnetohydrodynamic simulations of outflows from accretion disks. *Astrophys. J.* 439:L39–L42.
- Wardle, M. 1997. Magnetically driven winds from protostellar disks. In *ASP Conf. Ser. 121, Accretion Phenomena and Related Outflows*, eds. D. T. Wickramasinghe, G. V. Bicknell, and L. Ferrario (San Francisco: ASP), pp. 561–565.
- Wardle, M., and Königl, A. 1993. The structure of protostellar accretion disks and the origin of bipolar flows. *Astrophys. J.* 410:218–238.
- Weber, E. J., and Davis, L. 1967. The angular momentum of the solar wind. *Astrophys. J.* 148:217–227.